Proc. Natl. Acad. Sci. USA
Vol. 93, pp. 9850–9857, September 1996
Neurobiology

This contribution is part of the special series of Inaugural Articles by members of the National Academy of Sciences elected on April 30, 1996.

Fibroblast growth factor (FGF) homologous factors: New members of the FGF family implicated in nervous system development

PHILIP M. SMALLWOOD*†, IGNACIO MUNOZ-SANJUAN*, PATRICK TONG*‡, JENNIFER P. MACKE*†, STEWART H. C. HENDRY§, DEBRA J. GILBERT¶, NEAL G. COPELAND¶, NANCY A. JENKINS¶, AND JEREMY NATHANS*†‡§‖

*Departments of Molecular Biology and Genetics, §Neuroscience, and ‡Ophthalmology, and †Howard Hughes Medical Institute, Johns Hopkins University School of Medicine, Baltimore, MD 21205; and ¶Mammalian Genetics Laboratory, Advanced BioScience Laboratories–Basic Research Program, National Cancer Institute–Frederick Cancer Research and Development Center, Frederick, MD 21702

Contributed by Jeremy Nathans, July 3, 1996

ABSTRACT **Four new members of the fibroblast growth factor (FGF) family, referred to as fibroblast growth factor homologous factors (FHFs), have been identified by a combination of random cDNA sequencing, data base searches, and degenerate PCR. Pairwise comparisons between the four FHFs show between 58% and 71% amino acid sequence identity, but each FHF shows less than 30% identity when compared with other FGFs. Like FGF-1 (acidic FGF) and FGF-2 (basic FGF), the FHFs lack a classical signal sequence and contain clusters of basic residues that can act as nuclear localization signals. In transiently transfected 293 cells FHF-1 accumulates in the nucleus and is not secreted. Each FHF is expressed in the developing and adult nervous systems, suggesting a role for this branch of the FGF family in nervous system development and function.**

Fibroblast growth factors (FGFs) comprise a family of nine related polypeptides with broad mitogenic and cell survival activities (1–3). FGF-1 (acidic FGF) and FGF-2 (basic FGF), the first family members to be identified, purified, and sequenced, are widely expressed and are potent mitogens for a variety of cell types (4, 5). The gene encoding FGF-3 is a common target for activation by the mouse mammary tumor virus (6), and the genes encoding FGF-4, FGF-5, and FGF-6 have transforming activity when introduced into NIH 3T3 cells (7–9). FGF-7, FGF-8, and FGF-9 are mitogens for keratinocytes, mammary carcinoma cells, and astrocytes, respectively (10–12). Recent experiments indicate that several FGFs have bioactivities that were not evident during their initial identification. For example, FGF-2 can induce ventral mesoderm in *Xenopus* embryos (13, 14), FGF-4 is involved in growth and patterning of the chicken limb bud (15), FGF-5 controls hair follicle cycling in the mouse (16), and FGF-8 can cause duplications of the embryonic chicken midbrain (17).

The nine known FGFs are between 155 and 268 amino acid residues in length and share a conserved central region of ≈140 amino acids. This region forms a compact β-barrel with 3-fold symmetry that is nearly identical in structure to the folded core of interleukins-1α and -1β (18–21). FGF-1 and FGF-2 also resemble interleukin-1β in lacking a classical signal sequence. Current data indicate that FGF-1 and FGF-2 are released from cells by a route that is distinct from the endoplasmic reticulum–Golgi secretory pathway (22, 23).

FGF signaling is generally assumed to occur by activation of transmembrane tyrosine kinase receptors. Four FGF receptor (FGFR) genes have been identified thus far (24), and activating or inactivating receptor mutations have been described for a subset of these genes in both mice and humans. In the mouse, disruption of the FGFR1 or FGFR2 genes leads to early embryonic lethality (25, 26), and disruption of FGFR3 leads to bone overgrowth (27, 28). In humans, point mutations in FGFR1, FGFR2, and FGFR3 have been found in a variety of skeletal disorders (reviewed in ref. 29).

In this paper we report the identification and characterization of four new members of the FGF family, which we refer to as fibroblast growth factor homologous factors (FHFs). FHFs are expressed principally in the nervous system and are therefore likely to play a role in nervous system development and/or function.

MATERIALS AND METHODS

Random cDNA Sequencing. Details of retina cDNA library construction, template preparation, and sequence determination are reported in ref. 30.

Degenerate PCR. A fully degenerate sense-strand primer with a flanking *Eco*RI restriction site was synthesized for the amino acid sequence VFENYYV, and three partially degenerate antisense primers with a flanking *Bam*HI site were synthesized to include all possible codons for the amino acid sequence MKGN(H/R)VK. These primers were used to amplify human, murine, and bovine genomic DNA templates using *Thermus aquaticus* polymerase under the following conditions: 1× (94°C, 7 min), 35× (45°C, 2 min; 72°C, 0.5 min; 94°C 0.5 min; 95°C, 0.25 min). PCR products were cleaved with *Eco*RI and *Bam*HI, fractionated by preparative agarose gel electrophoresis, subcloned into pBluescript, and individually sequenced.

cDNA and Genomic Clones. Oligo(dT)-primed cDNA libraries from adult human retinas (31) and P0–P7 mouse eyes (A. Lanahan, H. Sun, and J.N., unpublished work) were screened by DNA hybridization under standard conditions (32). The complete coding region sequences of human FHF-1, FHF-2, and FHF-3 and mouse FHF-1, FHF-3, and FHF-4 were obtained from two independent cDNA clones. For human

Abbreviations: FGF, fibroblast growth factor; FGFR, FGF receptor, FHF, FGF homologous factor; RFLP, restriction fragment length polymorphism; ER, endoplasmic reticulum; cM, centimorgan; e, embryonic day; P, postnatal day; LGN, lateral geniculate nucleus; NLS, nuclear localization signal; β-gal, β-galactosidase; CNS, central nervous system.

Data deposition: The sequences reported in this paper have been deposited in the GenBank data base (accession nos. U66197–U66204).

‖To whom reprint requests should be addressed at: 805 PCTB, 725 North Wolfe Street, Johns Hopkins University School of Medicine, Baltimore, MD 21205. e-mail: jeremy.nathans@qmail.bs.jhu.edu.

FHF-4, the first 72 codons were sequenced from a single clone, and the rest of the coding region from two independent clones. For mouse FHF-2, the coding sequence was determined from cloned genomic DNA and from a PCR product obtained by amplification of the full-length coding region from the P0–P7 mouse eye cDNA library. A partial *Mbo*I digest mouse genomic DNA library in bacteriophage λ was screened to obtain the mouse FHF-2 genomic clones.

Chromosomal Localization. Human chromosome mapping was performed by Southern blot hybridization to DNA derived from a panel of 24 human/mouse or human/hamster hybrid cell lines, each carrying a different human chromosome (Oncor). Interspecific backcross progeny were generated by mating (C57BL/6J × *Mus spretus*)F_1 females and C57BL/6J males as described (33). A total of 205 N_2 mice were used to map the FHF loci. DNA isolation, restriction enzyme digestion, agarose gel electrophoresis, Southern blot transfer, and hybridization were performed essentially as described (34) using Zetabind nylon membrane (AMF Cuno). Washing was done to a final stringency of 0.8–1.0× SSCP/0.1% SDS at 65°C. The FHF-1 probe, a 1-kb fragment of mouse genomic DNA, detected fragments of 2.1 kb in C57BL/6J (B) DNA and 10.0 kb in *M. spretus* (S) DNA following digestion with *Bam*HI. The FHF-2 probe, a 0.75-kb fragment of mouse cDNA, detected *Bgl*I fragments of 19.0, 11.5, 8.2, and 2.2 kb (B) and 13.5, 8.2, and 2.2 kb (S). The FHF-4 probe, a 0.3-kb fragment of mouse cDNA, detected *Eco*RV fragments of ≈24.0 kb (B) and ≈7.7 kb (S).

Most of the probes and restriction fragment length polymorphisms (RFLPs) for the loci linked to the FHF genes in the interspecific backcross have been reported earlier. These include: Irg1 and Rap2a, on chromosome 14 (35); Smst on chromosome 16 (36); and Hprt, Cd401, and Ar on the X chromosome (37, 38). The probe for apolipoprotein D, a 290-bp *Hin*dIII/*Bam*HI fragment of rat cDNA, which was kindly provided by Alan Peterson, detected *Xba*I fragments of 3.1 and 2.8 kb (B) and 3.1 and 2.6 kb (S). The inheritance of the 2.6-kb *M. spretus*-specific *Xba*I RFLP was followed. Recombination distances were calculated as described in ref. 39 using the computer program SPRETUS MADNESS. Gene order was determined by minimizing the number of recombination events required to explain the allele distribution patterns.

RNase Protection. Total RNA was prepared from adult mouse brain, eye, heart, kidney, liver, lung, spleen, and testis by homogenization in guanidinium thiocyanate and extraction with phenol, followed by centrifugation through 5.7 M cesium chloride (32). Ten micrograms of total RNA from each tissue or 10 μg of yeast tRNA was used for the RNase protection assay. Riboprobes were synthesized using either T7 or T3 RNA polymerase on linearized templates in pBluescript. Each mouse FHF probe contained 150–250 bases from the antisense strand linked to 25–50 bases of vector sequence. Reagents were obtained from Ambion (Austin, TX), and the hybridization and digestion conditions were as recommended by Ambion.

***In Situ* Hybridization.** Freshly dissected adult mouse brains, whole embryos, or heads were rapidly frozen in plastic molds placed on a dry ice/ethanol slurry and processed for sectioning as described (40). ^{33}P-labeled antisense riboprobes were prepared from linearized pBluescript plasmid subclones using either T3 or T7 RNA polymerase. *In situ* hybridization was performed in 50% formamide/0.3 M NaCl at 56°C as described (41). Following RNase treatment, the slides were washed for 1 hr in 0.1× SSC at 55°C. After the hybridized sections were exposed to x-ray film, the slides were stained with cresyl violet. Digitized images of the stained slides and corresponding autoradiograms were superimposed using Adobe Photoshop software. The probes used were: FHF-1, 0.75 kb containing the complete coding region; FHF-2, 0.5 kb containing 0.3 kb of intron 4 and 0.2 kb of exon 5; FHF-3, two 0.4 kb segments containing the 5′ or 3′ halves of the coding region; FHF-4, 0.5 kb containing the 3′ two-thirds of the coding region. The coding regions of the different murine FHFs share between 63% and 71% nucleotide sequence identity, suggesting that there should be little or no cross-hybridization under the conditions used.

Immunohistochemistry. Rabbit polyclonal anti-FHF-1 antibodies were raised against a bacterial fusion protein consisting of the carboxyl-terminal 190 amino acids of FHF-1 fused to the T7 gene 10 protein (42). Anti-FHF-1 antibodies were affinity-purified using the fusion protein immobilized onto nitrocellulose; those antibodies directed against the fusion partner were removed by absorption to immobilized T7 gene 10 protein. For immunostaining of the primate brain, three monkeys (*Macaca mulatta*) were anesthetized with ketamine (35 mg/kg, i.m.), injected with a lethal dose of sodium pentobarbital (100 mg/kg, i.v.), and perfused through the heart with 4% paraformaldehyde in 0.1 M phosphate buffer (pH 7.4). The brains were removed, cryoprotected in 20% sucrose at 4°C, frozen, and cut at a thickness of 10 or 20 μm. Sections were sequentially incubated with affinity-purified rabbit anti-FHF-1 antibodies, biotinylated goat anti-rabbit IgG (Vector Laboratories), peroxidase-conjugated avidin (Extravidin, Sigma), and 3,3′-diaminobenzidine dihydrochloride (Aldrich) in the presence of hydrogen peroxide. Most sections were then mounted on gelatin-coated slides, dehydrated, cleared, and coverslipped. Following the histochemical reaction, some of the 10-μm thick sections were washed and then incubated sequentially in mouse anti-parvalbumin (Sigma), biotinylated horse anti-mouse IgG (Vector Laboratories), and streptavidin conjugated to Texas Red (Chemicon). These sections were mounted on clean slides, partially dried, and covered in a glycerol/phosphate buffer medium. Adjacent sections were processed histochemically for cytochrome oxidase or were stained for Nissl substance to determine the boundaries of subcortical nuclei or cortical areas and layers.

Production and Localization of FHF-1 in Transfected Cells. To increase the efficiency of FHF-1 translation, the region immediately 5′ of the initiator methionine coding was converted to an optimal ribosome binding site (CCACC**ATG**G) by PCR amplification, before inserting the complete FHF-1 open reading frame into the eukaryotic expression vector pCIS (43). The pCIS vector was also used for the β-galactosidase (β-gal) constructs. Human embryonic kidney cells (293) were transiently transfected with the expression construct and a plasmid expressing the simian virus 40 large T-antigen by the calcium phosphate method (43). For [^{35}S]methionine labeling cells were transferred to serum-free medium 24 hr after transfection, and labeled for 6 hr. For immunostaining, transfected cells were grown on gelatin-coated coverslips. One day after transfection the cells were fixed in 2% formaldehyde in PBS for 30 min at room temperature, permeabilized with cold methanol for 10 min at −20°C, preincubated for 15 min in 3% BSA in PBS, incubated for 1 hr at room temperature with affinity-purified anti-FHF-1 antibody at a dilution of 1:1000 and mouse monoclonal anti-BiP at a dilution of 1:400 in 3% BSA in PBS, washed 3 times for 15 min with 0.1% Tween 20 in PBS at room temperature, and then incubated with fluorescein-conjugated donkey anti-rabbit IgG and rhodamine-conjugated goat anti-mouse IgG in 3% BSA in PBS for 30–60 min. The coverslips were then washed in 0.1% Tween 20 in PBS and mounted in 0.1% 1,4-diazobicyclo[2.2.2]-octane, 75% glycerol, 10 mM Tris (pH 8.0). For 5-bromo-4-chloro-3-indolyl β-D-galactoside (X-Gal) staining, transfected cells were fixed in 0.5% glutaraldehyde/PBS for 10 min at room temperature, washed twice in PBS with 2 mM $MgCl_2$, incubated in 5 mM $K_3Fe(CN)_6$, 5 mM $K_4Fe(CN)_6$, 2 mM $MgCl_2$ in PBS for 1–2 hr at 37°C, and postfixed in 0.5% glutaraldehyde in PBS for 10 min at room temperature.

RESULTS

Identification of a Family of Sequences Homologous to the FGFs. In a pilot study aimed at identifying novel genes expressed in the retina, we obtained partial sequences from 5000 human

retina cDNA clones (ref. 30 and J.P.M., P.M.S., and J.N., unpublished work). One of the partial cDNA sequences, hereafter referred to as FHF-1, showed statistically significant homology to the FGFs. Full-length FHF-1 cDNA clones were isolated from an adult human retina cDNA library and were found to encode a protein of 244 amino acids with 27% amino acid identity to FGF-9, the most homologous member of the FGF family.

The FHF-1 sequence was used as a query to search the National Center for Biotechnology Information data base of expressed sequence tags and sequence tagged sites. One expressed sequence tag entry (DBEST ID 06895) derived from a human infant brain cDNA library (44), and hereafter referred to as FHF-2, encoded a segment of 77 amino acids with significant homology to the carboxyl terminus of FHF-1 but with no significant homology to other members of the FGF family. Similarly, one sequence tagged site entry (DBEST ID 76387; ref. 45), derived from human genomic DNA and hereafter referred to as FHF-3, contained a putative exon encoding a protein segment with a high degree of homology to FHF-1 and a low degree of homology to other FGF family members. Full-length FHF-2 and FHF-3 cDNA clones were isolated from an adult human retina cDNA library and found to encode proteins of 245 and 225 amino acids, respectively, with greater than 58% amino acid identity to FHF-1 and to each other.

To search for additional FHF-like sequences, degenerate oligonucleotide primers were designed for PCR amplification of codons 151–190 (in the FHF-1 numbering system) based on a comparison of the sequences of FHF-1, FHF-2, and FHF-3. An analysis of amplification products obtained using mouse, human, and bovine genomic DNA templates revealed that in each of these species this region of FHF-1, FHF-2, and FHF-3 is encoded within a single exon. This analysis also revealed a fourth class of FHF-like PCR products. cDNA clones encoding this fourth FHF family member, referred to as FHF-4, were obtained from a human retina cDNA library. The DNA sequences of these clones predict an encoded protein of 247 amino acids with greater than 60% amino acid identity to FHF-1, FHF-2, and FHF-3.

Fig. 1 shows an alignment of the amino acid sequences of human FHF-1, FHF-2, FHF-3, and FHF-4 with those of human FGF-1, FGF-2, and FGF-9. Also shown in Fig. 1 is a dendrogram of all the known FGF sequences, including the sequences of mouse FHF-1, FHF-2, FHF-3, and FHF-4. Pairwise comparisons between each FHF and the nine FGF family members show less than 30% amino acid identity, whereas all pairwise comparisons among the four FHFs show between 58 and 71% amino acid identity. Between mouse and human orthologues there is greater than 97% amino acid identity (see Fig. 1 legend). Thus, the four FHFs define a distinct and highly conserved branch of the FGF family.

As seen in Fig. 1, the four FHFs lack a recognizable amino-terminal signal sequence. Among the nine previously characterized members of the FGF family, FGF-1, FGF-2, and FGF-9 are also distinguished by the lack of a recognizable amino-terminal signal sequence (4, 5, 12). Current evidence indicates that FGF-1 and FGF-2 are synthesized in the cytosol and are released by a mechanism independent of the ER–Golgi secretory pathway (22, 23). Although FGF-9 lacks a cleavable amino-terminal signal sequence, it is glycosylated and efficiently secreted from cultured glioma, Chinese hamster ovary, and COS cells, presumably via the ER–Golgi pathway (12).

Intron–Exon Structure of the FHF-2 Gene. In the mouse, the FHF-2 gene is divided into five coding exons spread over at least 50 kb (Fig. 2*A*). The locations of the introns are indicated in Fig. 1 by arrowheads above the aligned amino acid sequences. By contrast, the genes encoding FGF-1, FGF-2, FGF-3, FGF-4, FGF-5, and FGF-6 are divided into three coding exons; in these genes the locations of the two introns correspond to the locations of introns 2 and 3 in the FHF-2 gene (Fig. 2*B*; refs. 6–9, 49, 50). The gene encoding FGF-8 also conforms to this arrangement but has two additional exons at the extreme 5′ end of the coding region (48).

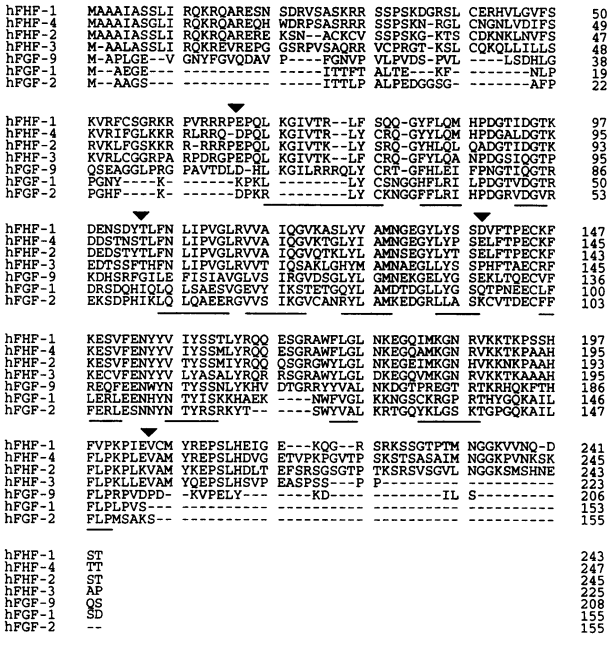

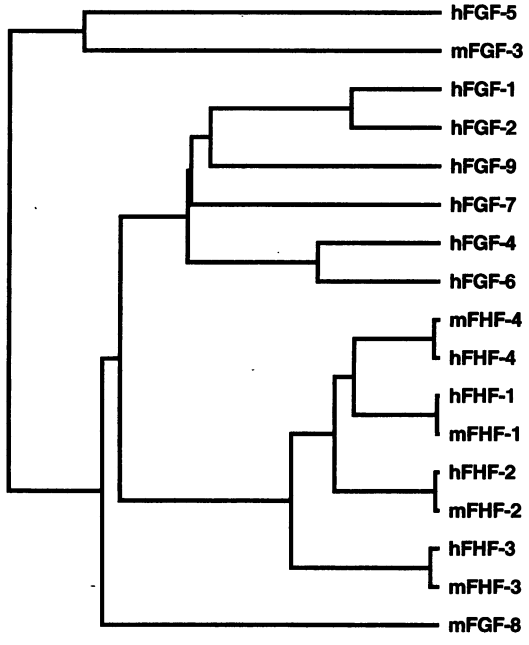

FIG. 1. Amino acid sequences of FHFs. (*Left*) Sequence alignment of the four human FHFs with human FGF-1, FGF-2, and FGF-9 using Geneworks software. The murine FHFs differ from their human orthologues by the amino acid substitutions listed below. The first and last letters indicate the amino acids in the human and mouse sequences, respectively, and the number indicates the position along the polypeptide chain. FHF-1: Q86E; FHF-2: A2T, L136H; FHF-3: A58T, P60Q, Q180R, L197V, Q207R, A217T, P225H; FHF-4: C40F, A181V, P221A, S244C. Intron locations for murine FHF-2 are indicated by arrowheads above the aligned sequences. If the adenosine of the initiator ATG is taken as nucleotide 1, then the FHF-2 introns are located after nucleotides 187, 298, 402, and 601. The locations of the 12 segments with β-sheet conformation in the FGF-2 crystal structure are underlined (20). Amino acid sequences of FGF-1, FGF-2, and FGF-9 are from refs. 12, 46, and 47. (*Right*) Dendrogram of mammalian FGF family members in which the length of each line is proportional to the degree of amino acid sequence divergence. h, human; m, murine.

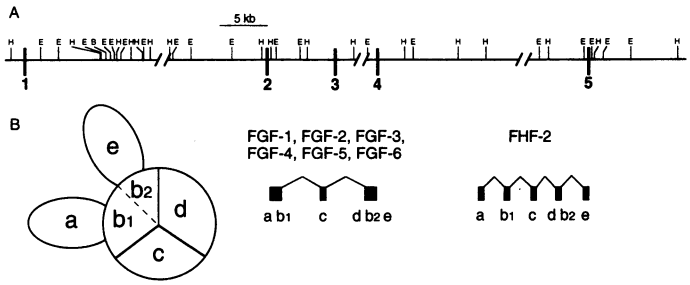

FIG. 2. Murine FHF-2 gene structure. (*A*) A restriction map derived from cloned mouse genomic DNA segments is shown with the locations of the five coding exons. Gaps separating the four cloned segments are of unknown size. B, *Bam*HI; E, *Eco*RI; H, *Hin*dIII. (*B*) Comparison of FGF-1 and FGF-2 tertiary structures (*Left*) and the intron–exon structures for FGF-1, FGF-2, FGF-3, FGF-4, FGF-5, and FGF-6 (*Center*) and FHF-2 (*Right*). The tertiary structure cartoon is based on the crystal structures of FGF-1 and FGF-2 (18–21), and is divided into a disordered amino-terminal domain (a), three structurally homologous folding units that make up a trigonal core (b–d), and a disordered carboxyl terminus (e). Folding unit b is formed from noncontiguous polypeptide segments, denoted b1 and b2. The FGF gene structures are reported in refs. 4, 6–9, and 48 and their associated GenBank entries.

Comparison of the FGF-1 and FGF-2 crystal structures with the FGF and FHF intron–exon structures shows that most introns demarcate boundaries between structural units. The FGF-1 and FGF-2 crystal structures (18–21) reveal five structural units as indicated schematically in Fig. 2*B*: a disordered amino terminus (unit a), an ordered central domain composed of three structurally homologous units arranged in a trigonal pyramid (units b–d), and a disordered carboxyl terminus (unit e). The disordered termini correspond to the regions of highest sequence divergence among FGF family members and in the FHF-2 gene these regions are encoded by the first and fifth exons. The second unit within the central domain (c) is encoded by the second exon in the FGF-1–FGF-6 genes and by the third exon in the FHF-2 gene. Three of 4 β-sheets that comprise the first folding unit within the central domain (b) are encoded by the second exon of the FHF-2 gene; the fourth β-sheet of this unit and the entire third unit of the central domain (d) are encoded by the fourth exon. This general correspondence between intron–exon structure and protein domains supports the hypothesis that exons evolved to encode distinct structural units (51).

Chromosomal Localization of FHFs. As a first step in the genetic analysis of the FHF subfamily, we have determined the chromosomal and subchromosomal localization of these genes. In humans, FHF-1, FHF-2, FHF-3, and FHF-4 are located on chromosomes 3, X, 17, and 13, respectively, as determined by Southern blot hybridization of genomic DNA from rodent–human hybrid cell lines carrying individual human chromosomes. The sequence tagged site described above, which encompasses one exon of FHF-3, was derived from human chromosome 17 and maps near the BRCA-1 gene (45).

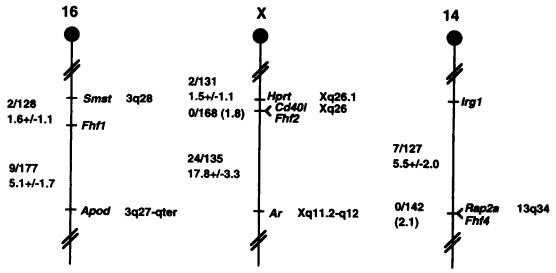

FIG. 3. Partial chromosome linkage maps showing the locations of the FHF-1, FHF-2, and FHF-3 genes in the mouse. The genes were mapped by interspecific backcross analysis. To the left of each chromosome map, the number of recombinant N_2 animals is presented divided by the total number of N_2 animals typed for each pair of loci. The recombination frequencies, expressed as genetic distance in cM (± 1 SEM) are also shown. The upper 95% confidence limit of the recombination distance is given in parentheses when no recombinants were found between loci. The positions of loci on human chromosomes, where known, are shown to the right of the chromosome maps. The map positions of most human loci can be obtained from the Genome Data Base, a computerized data base of human linkage information maintained by The William H. Welch Medical Library of The Johns Hopkins University.

The chromosomal locations of FHF-1, FHF-2, and FHF-4 in the mouse were determined using an interspecific backcross mapping panel from crosses of (C57BL/6J × *M. spretus*)F_1 × C57BL/6J. This mapping panel has been typed for over 2100 loci that are well distributed over all 19 mouse autosomes and the X-chromosome (33). C57BL/6J and *M. spretus* DNAs were digested with several different restriction enzymes and analyzed by Southern blot hybridization for informative RFLPs. The chromosomal location of each locus was determined by comparing its strain distribution in the backcross mice with the strain distribution patterns for all other loci already mapped in the backcross (Fig. 3). FHF-1 mapped to the proximal region of mouse chromosome 16, 1.6 centimorgans (cM) distal to Smst and 5.1 cM proximal to apolipoprotein D. FHF-2 mapped to the X chromosome and did not recombine with Cd401 in 168 mice typed in common, suggesting that the two loci are within 1.8 cM of each other (upper 95% confidence interval). FHF-4 mapped to the distal region of chromosome 14, and did not recombine with Rap2a in 142 mice typed in common, suggesting that the two loci are within 2.1 cM of each other. The FHF-3 gene was not mapped with the backcross panel because it failed to reveal an informative RFLP when tested with 14 restriction enzymes. The proximity of the human FHF-3 gene to BRCA-1 suggests that the mouse FHF-3 gene resides on chromosome 11 in the region that is syntenic with the BRCA-1 region of human chromosome 17. The FHF genes map in regions of the composite mouse linkage map (Mouse Genome Database, The Jackson Laboratory) that contain a number of mutations that may be candidate FHF alleles.

Expression Patterns of FHFs in the Mouse. In the adult mouse the tissue distribution of transcripts derived from each FHF gene was determined by RNase protection. Analysis of

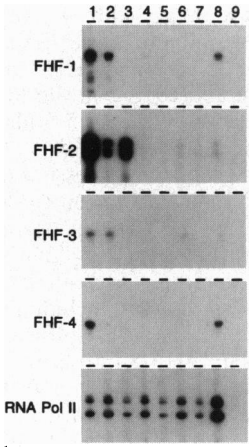

FIG. 4. Tissue distribution of FHF transcripts in the adult mouse. Ten micrograms of total RNA was used for RNase protection with the indicated FHF probes. A control reaction with an RNA polymerase II probe is shown at bottom. The RNA samples are as follows. Lanes: 1, brain; 2, eye; 3, heart; 4, kidney; 5, liver; 6, lung; 7, spleen; 8, testis; 9, yeast tRNA.

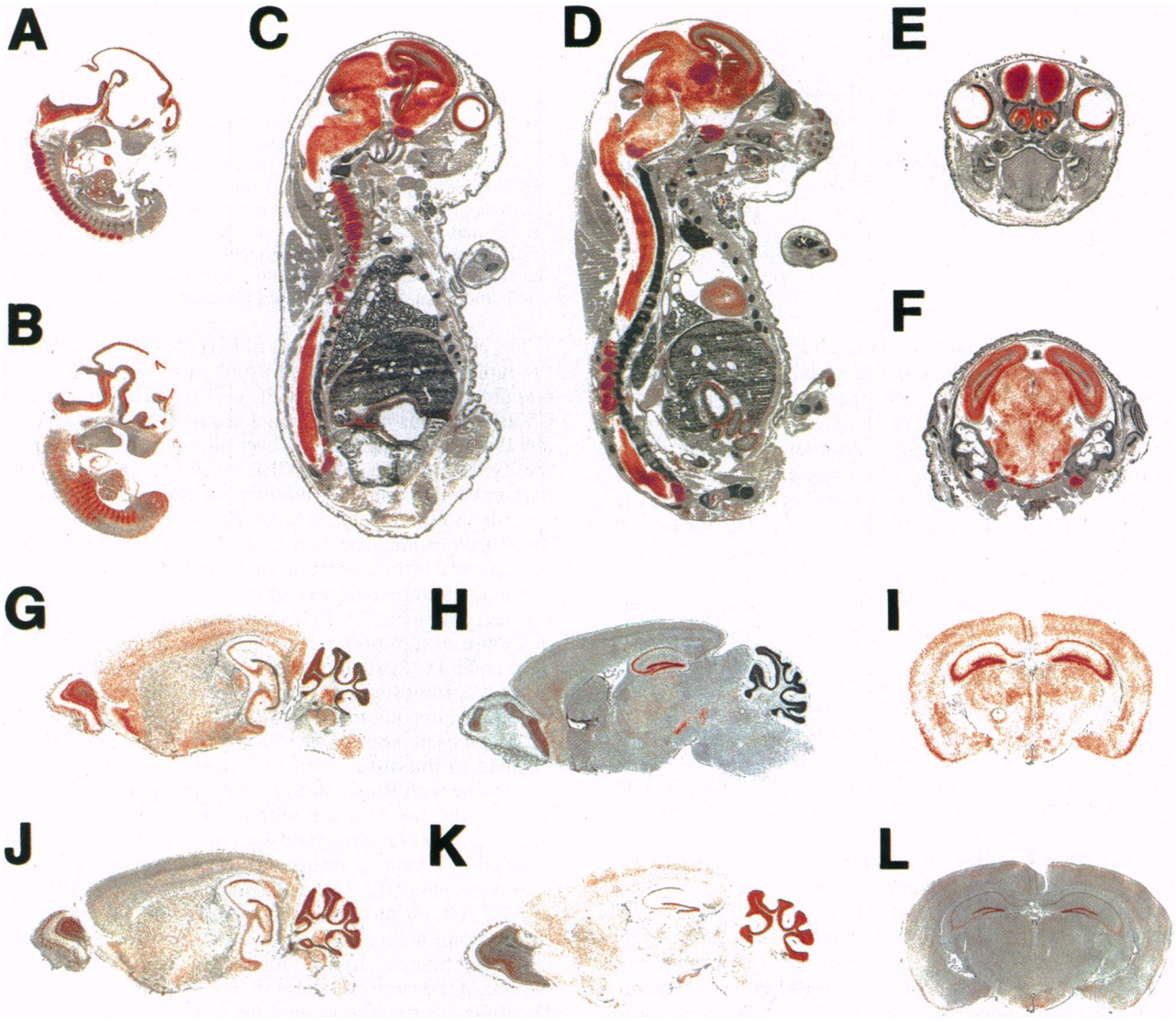

FIG. 5. *In situ* localization of FHF transcripts in the developing and adult mouse. ^{33}P *in situ* hybridization is shown in red superimposed upon a cresyl violet stain shown in black and white. (*A*) FHF-2, e11; (*B*) FHF-3, e11; (*C* and *D*) FHF-2, e17; (*E*) FHF-1, P1, coronal section through the head at the level of the eyes; (*F*) FHF-2, P1, coronal section through the center of the head; (*G*) FHF-1, adult; (*H* and *I*) FHF-2, adult; (*J*) FHF-3, adult. (*K* and *L*) FHF-4, adult.

RNA from brain, eye, heart, kidney, liver, lung, spleen, and testis revealed expression of each FHF in the brain, and expression of FHF-1, FHF-2, and FHF-3 in the eye; FHF-1 and FHF-4 in the testis; and FHF-2 in the heart (Fig. 4). In the brain, FHF-2 transcripts are at least 5-fold more abundant than transcripts from any of the other FHFs.

The patterns of FHF gene expression during development were studied by *in situ* hybridization to sections obtained on embryonic day 11 (e11) and 17 (e17), postnatal day 1 (P1), and from adults. FHF-2 transcripts are abundant at each of the times examined, and are present in all divisions of the central and peripheral nervous systems, including the enteric nervous system (Fig. 5 *A*, *C*, *D*, and *F*). Consistent with the RNase protection experiment, FHF-2 transcripts were also observed in the developing heart at e17 (Fig. 5*D*). FHF-1, FHF-3, and FHF-4 transcripts are also widely distributed throughout the developing nervous system (Fig. 5 *B* and *E* and data not shown). For example, at P1, FHF-1 is highly expressed in the retina, olfactory epithelium, and olfactory bulb (Fig. 5*E*). At e11, FHF-1 and FHF-3 are also found in a segmental pattern in the body wall (Fig. 5*B* and data not shown). In the adult brain each FHF shows a distinctive pattern of expression: FHF-1 transcripts are present at high levels in the olfactory bulb and at lower levels in the cerebellum, the deep cerebellar nuclei, throughout the cortex, and in multiple midbrain structures (Fig. 5*G*); FHF-2 transcripts are most abundant in the hippocampus and are present at lower levels in multiple brain areas (Fig. 5 *H* and *I*); FHF-3 transcripts are present in the olfactory bulb, hippocampus, and cerebellum where they are most concentrated in the Purkinje cell layer (Fig. 5*J*); and FHF-4 transcripts are present at high levels throughout the granular layer of the cerebellum and at lower levels in the hippocampus and olfactory bulb (Fig. 5 *K* and *L*).

Distribution of FHF-1 Immunoreactivity in Monkey Brain. The distribution of FHF-1 immunoreactivity in the adult rhesus monkey brain was examined using affinity-purified polyclonal anti-FHF-1 antibodies. These antibodies bind to recombinant FHF-1 but do not bind to recombinant FHF-2, as determined by immunostaining of transfected 293 cells and by Western blotting; their binding to FHF-3 and FHF-4 has not been tested. Although we refer to immunoreactivity with these antibodies as "FHF-1 immunoreactivity," the possibility exists that other members of the FHF family are in part responsible for the observed immunostaining.

FHF-1 immunoreactive somata are present throughout the rhesus monkey cerebral cortex, but these are unevenly distrib-

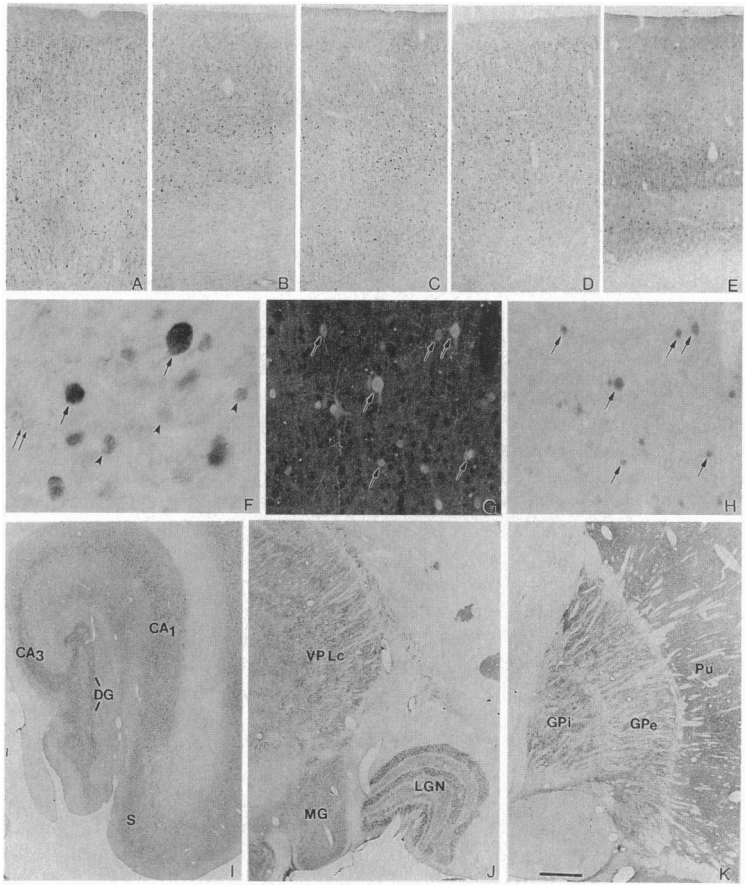

FIG. 6. FHF-1 immunostaining in the macaque monkey CNS. (*A*) Precentral motor cortex; (*B*) area 3b in the primary somatosensory cortex; (*C*) primary auditory cortex; (*D*) area 7b in the superior perietal lobule; (*E*) primary visual cortex; (*F–H*) populations of cortical neurons immunoreactive for FHF-1 include large intensely immunoreactive cells (arrows), small weakly immunoreactive cells (arrowheads), and small weakly immunoreactive cells with fine processes resembling microglia (double arrows). Simultaneous immunostaining for parvalbumin (*G*) and FHF-1 (*H*) shows that large and small neurons are immunoreactive for both. An uneven distribution of FHF-1 immunoreactive somata is seen in the hippocampal formation (*I*), including the subicular complex (S), the CA fields, and the dentate gyrus (DG). In the dorsal thalamus (*J*), FHF-1 immunoreactive somata occupy patches in the caudal ventroposteriolateral nucleus and are found in both magnocellular and parvocellular layers of the LGN. The medial geniculate complex contains few immunostained cells. In the basal telencephalon (*K*), immunoreactive neurons are present in both the external and internal segments of the globus pallidus (Gpe and GPi). (Scale bars = 500 μm in *A–E*, 20 μm in *F*, 75 μm in *G* and *H*, and 1 mm in *I–K*.)

uted across layers in any one area and display marked variations in density and distribution across functional areas (Fig. 6 *A–E*). The low magnification photomicrographs in Fig. 6 show that in primary visual, somatosensory, and auditory areas a relatively high density of immunostained cells is present and these occupy predominantly the middle layers. In contrast, fewer and more widely scattered immunostained neurons are present in the precentral motor area and in the association cortex of the superior parietal lobule.

Common to each of these cortical areas is the presence of several FHF-1 immunoreactive populations, the most prominent of which have relatively large (12–14-μm diameter), intensely immunoreactive somata. Other neurons with smaller (8–10-μm diameter) and more lightly immunostained somata are also present in all areas (Fig. 6*F*). Colocalization experiments demonstrate that the FHF-1 immunoreactive neurons in the cerebral cortex make up a subpopulation of neurons immunoreactive for the calcium binding protein, parvalbumin (Fig. 6 *G* and *H*), which have previously been shown to comprise a subset of GABAergic interneurons in the monkey cerebral cortex (52). Variations in immunostained cell density are also seen in the hippocampal formation where intensely immunoreactive somata are relatively common in the subicular complex but are widely scattered in the CA fields, the dentate hilus, and the dentate gyrus (Fig. 6*I*).

A different pattern of FHF-1 immunostaining is seen in the dorsal thalamus (Fig. 6*J*). Only a few of the many nuclei in this region contain immunoreactive neurons; most prominent among them is the principal somatosensory relay nucleus (the caudal ventroposteriolateral nucleus) and the visual relay nucleus (the lateral geniculate nucleus, LGN). In the LGN both magnocellular and parvocellular layers are equally immunostained. Fig. 6*J* shows that in the LGN ipsilateral to an eye deprived by occlusion since birth, FHF-1 immunostaining is markedly lower in layers innervated by the deprived eye than in layers innervated by the normal eye.

The relatively large size of FHF-1 immunostained somata in nuclei of the dorsal thalamus suggests they are cell bodies of neurons that send their axons to the cerebral cortex. Localization of FHF-1 immunoreactivity in neurons of caudal ventroposteriolateral nucleus and LGN that are lightly immunoreactive for parvalbumin (data not shown) supports such a conclusion, because these parvalbumin immunostained neurons in dorsal thalamus have been shown to be thalamocortical neurons (53).

Outside of the dorsal thalamus FHF-1 immunoreactive neurons are present in a diverse collection of subcortical nuclei, including the globus pallidus and putamen, red nucleus, substantia nigra, and third nerve complex (Fig. 6*K* and data

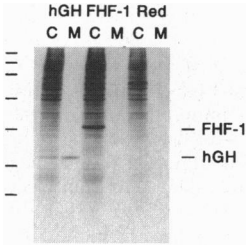

FIG. 7. FHF-1 is not secreted by human embryonic kidney (293) cells. 293 cells were transiently transfected with expression plasmids directing the synthesis of human growth hormone (*Left*), FHF-1 (*Middle*), or the human red cone pigment (*Right*). The cells were labeled for 6 hr with [^{35}S]methionine in serum-free medium, and the total protein present in the cells (C) or medium (M) was resolved by SDS/PAGE and visualized by autoradiography. Secretion of human growth hormone (hGH), but not FHF-1, is observed. The mobilities of protein standards are indicated at the left; from top to bottom their molecular masses (in kDa) are: 220, 97, 66, 46, 30, 21.5, and 14.3. The mobilities of hGH and FHF-1 are indicated to the right.

not shown). In addition, large cells in the deep layers of both the superior and inferior colliculi are immunostained, as are neurons in the deep cerebellar nuclei. In conclusion, FHF-1 immunoreactivity is broadly distributed across the neuraxis but at each level is present in subsets of neurons.

Subcellular Localization of FHF-1 in Transfected Cells. As noted above, of the nine FGFs described prior to this report, FGF-1 and FGF-2 are distinguished by the lack of an amino-terminal signal sequence and by secretion via a pathway that is independent of the ER and Golgi apparatus (22, 23). Moreover, FGF-1 and a subset of FGF-2 isoforms (produced by alternative translation initiation) have been shown to accumulate in the nuclei of the cells in which they are synthesized as well as in the nuclei of target cells (54–59). These proteins contain a nuclear localization signal (NLS) that conforms closely to a consensus NLS. The nuclear accumulation of FGF-1 and the FGF-2 isoforms has raised the possibility that these proteins may have modes of action in addition to those mediated by binding and activation of cell surface receptors.

Like FGF-1 and FGF-2, each FHF both lacks a classical signal sequence and contains clusters of basic residues near its amino terminus that could serve as an NLS. These data suggest that the FHFs may resemble FGF-1 and FGF-2 in their mechanism of secretion and in their subcellular localization. To test this possibility, we determined the fate of FHF-1 synthesized in transiently transfected human embryonic kidney (293) cells. In one set of experiments, biosynthetically labeled FHF-1 was found to accumulate to high levels intracellularly but was not detectably secreted into the medium (Fig. 7). By contrast, human growth hormone produced in parallel transfections was efficiently secreted. As 293 cells can secrete a wide variety of growth factors through the ER–Golgi pathway, this experiment is consistent with the idea that the FHFs are not secreted via this route.

In a second set of experiments immunostaining of transfected 293 cells revealed accumulation of FHF-1 in the nucleus (Fig. 8*A*), suggesting that the clusters of basic residues can function as an NLS. A similar result was obtained with FHF-2 (data not shown). Two main classes of NLS motifs have been described, the classical and bipartite (60). The classical NLS contains a cluster of 6 lysine or arginine residues, and the bipartite NLS contains 2 clusters of 3 or 4 basic residues separated by a 10 amino acid spacer. In FHF-1 the clusters of basic residues resemble more closely the bipartite NLS consensus. To identify and characterize the putative FHF-1 NLS, we determined the subcellular localization of deletion mutants of FHF-1 by immunostaining with anti-FHF-1 antibodies, and of fusions between FHF-1 and β-gal by X-gal staining. These experiments show that the two clusters of arginines and lysines at amino acids 11–18 and 28–38 comprise the two basic regions of a bipartite NLS. In the context of the FHF-1 protein, deletion of either cluster produced a modest increase in the level of cytoplasmic FHF-1 but left significant nuclear accumulation (constructs 2 and 3), whereas deletion of both regions abolished nuclear accumulation (Fig 8*B*, construct 4). To further characterize the minimal region required for import, the first 56 or the first 69 residues of FHF-1 were fused to β-gal and shown to contain a functional NLS (Fig. 8 *C–F*, constructs 5 and 6). Fusion of FHF-1 residues 1–22 or 23–55 individually to β-gal failed to direct nuclear localization, indicating a requirement for both parts of the bipartite NLS or for sequences distal to the first 55 residues. With β-gal fused to the first 69 amino acids of FHF-1, the results of deletion analysis resembled those seen with intact FHF-1 (constructs 5, 9, 10, and 11). Finally, fusion of FHF-1 residues 11–38, containing only the two clusters of basic residues separated by a 10 amino acid spacer, conferred nuclear localization, although less efficiently than the larger segments that contained this region, suggesting that residues 1–10 or 56–68, outside of the bipartite NLS consensus, may play an ancillary role in nuclear localization.

DISCUSSION

In this report we present the cloning and initial characterization of four FHFs that together define a new branch of the FGF family. This work brings to 13 the number of known FGF family members. The FHFs share ≈30% amino acid identity with previously characterized FGFs, a degree of relatedness typical of most pairwise comparisons between FGF family members. The high degree of sequence diversity among known FGFs in part reflects the independent routes by which these factors were identified. With the exception of FGF-6, each of the previously described FGF family members was identified without using probes or sequence information derived from other family members.

The expression of each FHF is highly restricted during development and in the adult, being confined primarily to the nervous system. In the adult mouse brain, *in situ* hybridization reveals

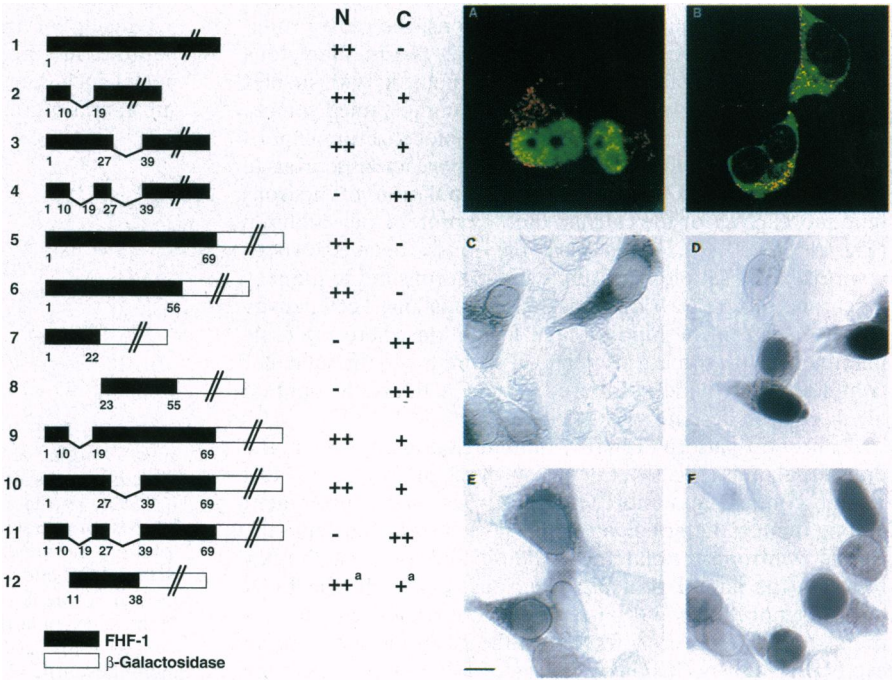

FIG. 8. Identification of a NLS in FHF-1. (*Left*) Summary of the FHF-1 constructs and their localization by immunostaining (constructs 1–4) or FHF-1–β-gal fusions and their localization by X-Gal staining (constructs 5–12). The numbers underneath each construct indicate the amino acids from FHF-1 that are present in that construct. (*Right*) (*A* and *B*) Double-label immunofluorescent localization of FHF-1 (green) and BiP (an ER marker, red) optically sectioned at 0.7 μm. (*C–F*) Histochemical localization of FHF-1–β-gal fusion proteins. All experiments were performed with transiently transfected 293 cells. (*A*) Full-length FHF-1, construct 1; (*B*) construct 4; (*C*) full-length β-gal; (*D*) construct 6; (*E*) construct 11; (*F*) construct 12. ++, strong staining; +, weak staining; −, no staining. "a," construct 12 shows cytoplasmic staining in 15–20% of cells and nuclear localization in 80–85% of cells.

distinctive patterns of expression of each FHF, and in the adult rhesus monkey brain, immunostaining with anti-FHF-1 antibodies reveals immunoreactivity within neurons in a wide variety of central nervous system (CNS) regions. If the FHFs resemble other FGFs in acting as local growth or survival factors then we would predict that they act on cell types within the CNS, i.e. neurons, glia, and/or cells of the vasculature.

The pathway(s) of FHF biosynthesis and the mechanisms by which the FHFs act are currently unknown, but it is reasonable to suppose that they will resemble those of other FGFs. Thus, we presume that high-affinity transmembrane receptors exist to transduce FHF signals and that extracellular matrix molecules such as heparin act as co-ligands for receptor binding. Similarities between the sequences of the FHFs and of FGF-1 and FGF-2 suggest additional similarities in those properties that are peculiar to FGF-1 and FGF-2. In particular, the absence of an amino-terminal signal sequence in all FHFs and the observed lack of FHF-1 secretion from transfected 293 cells, suggests that, like FGF-1 and FGF-2, the FHFs may be released from cells by a mechanism that is independent of the ER–Golgi secretory pathway. Whether such an alternative release pathway is activated by specific stimuli, as observed for the pathway of interleukin-1β release (61), or is present in only some cell types, remains to be determined. Similarly, the presence of a functional NLS in FHF-1 and of NLS-like sequences in FHF-2, FHF-3, and FHF-4 suggests that the FHFs, like FGF-1 and FGF-2, may normally enter the nucleus, a possibility supported by the localization of FHF-1 immunoreactivity to both the nucleus and cytoplasm of neurons within the primate CNS. Although the relevance of nuclear accumulation to FHF action remains to be determined, recent experiments suggest that mitogenic activity of FGF-1 requires a functional NLS (54, 59).

The preceeding discussion suggests that the FHFs may play important roles in nervous system development, function, and disease. Moreover, the evolutionary conservation of FHF orthologues suggests that each FHF has distinct and conserved biological activities. The identification and characterization of these activities will require both the development of assays for FHF action *in vitro* and targeted manipulations of FHF gene structure *in vivo*. Once these activities are identified, it may be possible to produce biological effects of therapeutic value by either augmenting or antagonizing FHF action.

We thank Clark Riley, Carol Davenport, Jeanine Ptak, and Lisa Eiben for sequencing and oligonucleotide synthesis; K. Andreasson and M. Papapavlou for help with tissue preparation and advice on *in situ* hybridization; T. Lanahan and S.-J. Lee for mouse cDNA and genomic DNA libraries; J. Borjigin for the hGH plasmid; C. Machamer for anti-BiP antibodies; B. Cho, M. Barnstead, and D. Householder for excellent technical assistance; and Paul Worley and Randall Reed for helpful comments on the manuscript. This research was supported by the Ruth and Milton Steinbach Fund, the Howard Hughes Medical Institute, and the National Cancer Institute, Department of Health and Human Services, under contract with Advanced BioScience Laboratories.

1. Burgess, W. H. & Maciag, T. (1989) *Annu. Rev. Biochem.* **58,** 575–606.
2. Baird, A. & Klagsbrun, M., eds. (1991) *Ann. N.Y. Acad. Sci.* **638.**
3. Eckenstein, F. P. (1994) *J. Neurobiol.* **25,** 1467–1480.
4. Abraham, J. A., Mergia, A., Whang, J. L., Tumolo, A., Friedman, J., Hjerrild, K. A., Gospodarowicz, D. & Fiddes, J. C. (1986) *Science* **233,** 545–548.
5. Jaye, M., Howk, R., Burgess, W., Ricca, G. A., Chiu, I. M., Ravera, M. W., O'Brien, S. J., Modi, W. S., Macaig, T. & Drohan, W. N. (1986) *Science* **233,** 541–545.
6. Moore, R., Casey, G., Brookes, S., Dixon, M., Peters, G. & Dickson, C. (1986) *EMBO J.* **5,** 919–924.
7. Yoshida, T., Miyagawa, K., Odagiri, H., Sakamoto, H., Little, P. F. R., Terada, M. & Sugimura, T. (1987) *Proc. Natl. Acad. Sci. USA* **84,** 7305–7309.
8. Zhan, X., Bates, B., Hu, X. & Goldfarb, M. (1988) *Mol. Cell. Biol.* **8,** 3487–3495.
9. Marics, I., Adelaide, J., Raybaud, F., Mattei, M.-G., Coulier, F., Planche, J., de Lapeyriere, O. & Birnbaum, D. (1989) *Oncogene* **4,** 335–340.
10. Finch, P. W., Rubin, J. S., Miki, T., Ron, D. & Aaronson, S. A. (1989) *Science* **245,** 752–755.
11. Tanaka, A., Miyamoto, K., Minamino, N., Takeda, M., Sato, B., Matsuo, H. & Matsumoto, K. (1992) *Proc. Natl. Acad. Sci. USA* **89,** 8928–8932.
12. Miyamoto, M., Naruo, K.-I., Seko, C., Matsumoto, S., Kondo, T. & Kurokawa, T. (1993) *Mol. Cell. Biol.* **13,** 4251–4259.
13. Slack, J. M. W., Darlington, B. G., Heath, J. K. & Godsave, S. F. (1987) *Nature (London)* **326,** 197–200.
14. Kimmelman, D. & Kirschner, M. (1987) *Cell* **51,** 869–877.
15. Niswander, L., Jeffrey, S., Martin, G. R. & Tickle, C. (1994) *Nature (London)* **371,** 609–612.
16. Hebert, J. M., Rosenquist, T., Gotz, J. & Martin, G. (1994) *Cell* **78,** 1017–1025.
17. Crossley, P. H., Martinez, S. & Martin, G. R. (1996) *Nature (London)* **380,** 66–68.
18. Zhu, X., Komiya, H., Chirino, A., Faham, S., Fox, G. M., Arakawa, T., Hsu, B. T. & Rees, D. C. (1991) *Science* **251,** 90–93.
19. Zhang, J., Cousens, L. S., Barr, P. J. & Sprang, S. R. (1991) *Proc. Natl. Acad. Sci. USA* **88,** 3446–3450.
20. Eriksson, E. A., Cousens, L. S., Weaver, L. H. & Mathews, B. W. (1991) *Proc. Natl. Acad. Sci. USA* **88,** 3441–3445.
21. Ago, H., Kitagawa, Y., Fujishima, A., Matsuura, Y. & Katsube, Y. (1991) *J. Biochem.* **110,** 360–363.
22. Florkiewicz, R. Z., Majack, R. A., Buechler, R. D. & Florkiewicz, E. (1995) *J. Cell. Physiol.* **162,** 388–399.
23. Jackson, A., Tarantini, F., Gamble, S., Friedman, S. & Macaig, T. (1995) *J. Biol. Chem.* **270,** 33–36.
24. Johnson, D. E. & Williams, L. T. (1993) *Adv. Cancer Res.* **60,** 1–41.
25. Deng, C.-X., Wynshaw-Boris, A., Shen, M. M., Daugherty, C., Ornitz, D. M. & Leder, P. (1994) *Genes Dev.* **8,** 3045–3057.
26. Yamaguchi, T. P., Harpal, K., Henkemeyer, M. & Rossant, J. (1994) *Genes Dev.* **8,** 3032–3044.
27. Deng, C., Wynshaw-Boris, A., Zhou, F., Kuo, A. & Leder, P. (1996) *Cell* **84,** 911–921.
28. Colvin, J. S., Bohne, B. A., Harding, G. W., McEwen, D. G. & Ornitz, D. M. (1996) *Nat. Genet.* **12,** 390–397.
29. Muenke, M. & Schell, U. (1995) *Trends Genet.* **11,** 308–313.
30. Wang, Y., Macke, J. P., Abella, B. S., Andreasson, K., Worley, P., Gilbert, D. J., Copeland, N. G., Jenkins, N. A. & Nathans, J. (1996) *J. Biol. Chem.* **271,** 4468–4476.
31. Nathans, J., Thomas, D. & Hogness, D. S. (1986) *Science* **232,** 193–202.
32. Sambrook, J., Fritsch, E. F. & Maniatis, T. (1989) *Molecular Cloning: A Laboratory Manual* (Cold Spring Harbor Lab. Press, Plainview, NY), 2nd Ed.
33. Copeland, N. G. & Jenkins, N. A. (1991) *Trends Genet.* **7,** 113–118.
34. Jenkins, N. A., Copeland, N. G., Taylor, B. A. & Lee, B. K. (1982) *J. Virol.* **43,** 26–36.
35. Lee, C. G. L., Jenkins, N. A., Gilbert, D. J., Copeland, N. G. & O'Brien, W. E. (1995) *Immunogenetics* **41,** 263–270.
36. Siracusa, L. D., Jenkins, N. A. & Copeland, N. G. (1991) *Genetics* **127,** 169–179.
37. Allen, R. C., Armitage, R. J., Conley, M. E., Rosenblatt, H., Jenkins, N. A., Copeland, N. G., Bedell, M. A., Edelhoff, S., Disteche, C. M., Simoneaux, D. K., Fanslow, W. C., Belmont, J. I. & Spriggs, M. K. (1993) *Science* **259,** 990–993.
38. Fletcher, F. A., Renshaw, B., Hollingsworth, T., Baum, P., Lyman, S. D., Jenkins, N. A, Gilbert, D. J., Copeland, N. G. & Davison, B. L. (1994) *Genomics* **24,** 127–132.
39. Green, E. L. (1981) *Genetics and Probability in Animal Breeding Experiments* (Oxford Univ. Press, New York), pp. 77–113.
40. Cole, A., Abu-Shakra, S., Saffen, D., Baraban, J. & Worley, P. (1990) *J. Neurochem.* **55,** 1920–1927.
41. Saffen, D., Cole, A., Worley, P., Christy, B., Ryder, K. & Baraban, J. (1988) *Proc. Natl. Acad. Sci. USA* **85,** 7795–7799.
42. Studier, F. W., Rosenberg, A. H., Dunn, J. J. & Dubendorf, J. W. (1980) *Methods Enzymol.* **185,** 60–89.
43. Gorman, C. M., Gies, D. R. & McCray, G. (1990) *DNA Protein Eng. Technol.* **2,** 3–10.
44. Adams, M. D., Soares, M. B., Kerlavage, A. R., Fields, C. & Venter, J. C. (1993) *Nat. Genet.* **4,** 373–380.
45. Brody, L., Abel, K. J., Castilla, L. H., Couch, F. J., McKinley, D. R., Yin, G. Y., Ho, P. P., Merajver, S., Chandrasekharappa, S. C., Xu, J., Cole, J. L., Struewing, J. P., Valdes, J. M., Collins, F. S. & Weber, B. L. (1995) *Genomics* **25,** 238–247.
46. Yu, Y.-L., Kha, H., Goldin, J. A., Migchielsen, A. A. J., Goetzl, E. J. & Turck, C. W. (1992) *J. Exp. Med.* **175,** 1073–1080.
47. Prats, H., Kaghad, M., Prats, A. C., Klagsbrun, M., Lelias, J. M., Liauzun, P., Chalon, P., Tauber, J. P., Amalric, F., Smith, J. A. & Caout, D. (1989) *Proc. Natl. Acad. Sci. USA* **86,** 1836–1840.
48. Tanaka, A., Miyamoto, K., Matsuo, H., Matsumoto, K. & Yoshida, H. (1995) *FEBS Lett.* **363,** 226–230.
49. Abraham, J. A., Whang, J. L., Tumolo, A., Mergia, A., Friedman, J., Gospodarowicz, D. & Fiddes, J. C. (1986) *EMBO J.* **5,** 2523–2528.
50. Mergia, A., Tischer, E., Graves, D., Tumolo, A., Miller, J., Gospodarowicz, D., Abraham, J. A., Shipley, G. D. & Fiddes, J. C. (1989) *Biochem. Biophys. Res. Commun.* **164,** 1121–1129.
51. Gilbert, W. (1978) *Nature (London)* **271,** 501.
52. Hendry, S. H. C., Jones, E. G., Emson, P. C., Lawson, D. E. M., Heizmann, C. W. & Streit, P. (1989) *Exp. Brain Res.* **76,** 467–472.
53. Jones, E. G. & Hendry, S. H. C. (1989) *Eur. J. Neurosci.* **1,** 222–246.
54. Imamaura, T., Engleka, K., Zhan, X., Tokita, Y., Forough, R., Roeder, D., Jackson, A., Maier, J. A. M., Hla, T. & Maciag, T. (1990) *Science* **249,** 1567–1570.
55. Imamaura, T., Tokita, Y. & Matsui, Y. (1992) *J. Biol. Chem.* **267,** 5676–5679.
56. Bugler, B., Amalric, F. & Prats, H. (1991) *Mol. Cell. Biol.* **11,** 573–577.
57. Zhan, X., Hu, X., Friedman, S. & Macaig, T. (1992) *Biochem. Biophys. Res. Commun.* **188,** 982–991.
58. Cao, Y., Ekstrom, M. & Petterson, R. F. (1993) *J. Cell Sci.* **104,** 77–87.
59. Wiedlocha, A., Falnes, P. O., Madshus, I. H., Sandvig, K. & Olsnes, S. (1994) *Cell* **76,** 1039–1051.
60. Boulikas, T. (1993) *Crit. Rev. Eukaryotic Gene Expression* **3,** 193–227.
61. Hogquist, K. A., Nett, M. A., Unanue, E. R. & Chaplin, D. D. (1991) *Proc. Natl. Acad. Sci. USA* **88,** 8485–8489.